Supporting Information

Evaluation of the Interaction Parameter for Poly(solketal methacrylate)-*block*-polystyrene Copolymers

Duk Man Yu[†], Jose Kenneth D. Mapas[‡], Hyeyoung Kim[†], Jaewon Choi[†], Alexander E. Ribbe[†], Javid Rzayev*[,‡], Thomas P. Russell*[,†,§,∥]

[†]Department of Polymer Science and Engineering, University of Massachusetts Amherst, 120 Governors Drive, Amherst, Massachusetts 01003, United States

[‡]Department of Chemistry, University at Buffalo, The State University of New York, Buffalo, New York 14260-3000, United States

[§]Materials Science Division, Lawrence Berkeley National Laboratory, 1 Cyclotron Road, Berkeley, California 94720, United States

[∥]Beijing Advanced Innovation Center for Soft Matter Science and Engineering, Beijing University of Chemical Technology, Beijing 100029, China

Corresponding Authors

*E-mail: jrzayev@buffalo.edu, Tel.: (716) 645-4314, Fax: (716) 645-6963

*E-mail: russell@mail.pse.umass.edu, Tel.: (413) 577 1516, Fax: (413) 577-1510

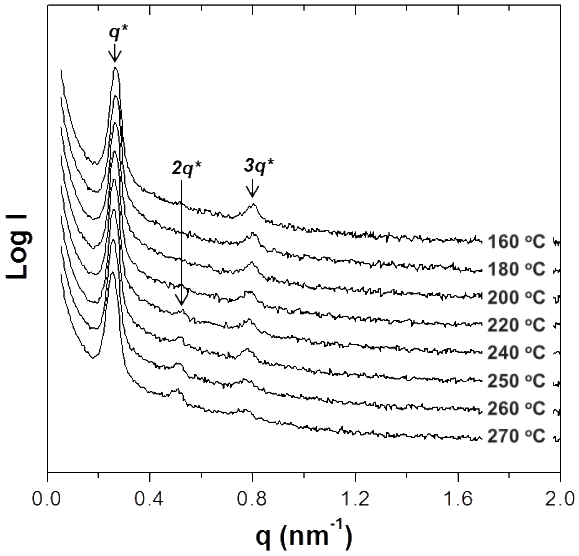

Figure S1. SAXS absolute intensity profiles for pristine P(SM21-S22) (N = 316) at various temperatures with a heating rate of 1.0 °C/min. The temperature-dependent profiles are vertically shifted in the range of 160 °C to 270 °C. The primary (q*) and higher order reflections (3q*) of the lamellar structure were observed. The second order peak (2q*) appeared from 240 °C because of the increase in asymmetric lamellar microdomains by thermal energy. Until 270 °C, the intensity at q* was not changed, indicating that P(SM21-S22) does not show a phase-mixed state and also maintains the condition of $\chi N > 10.5$.

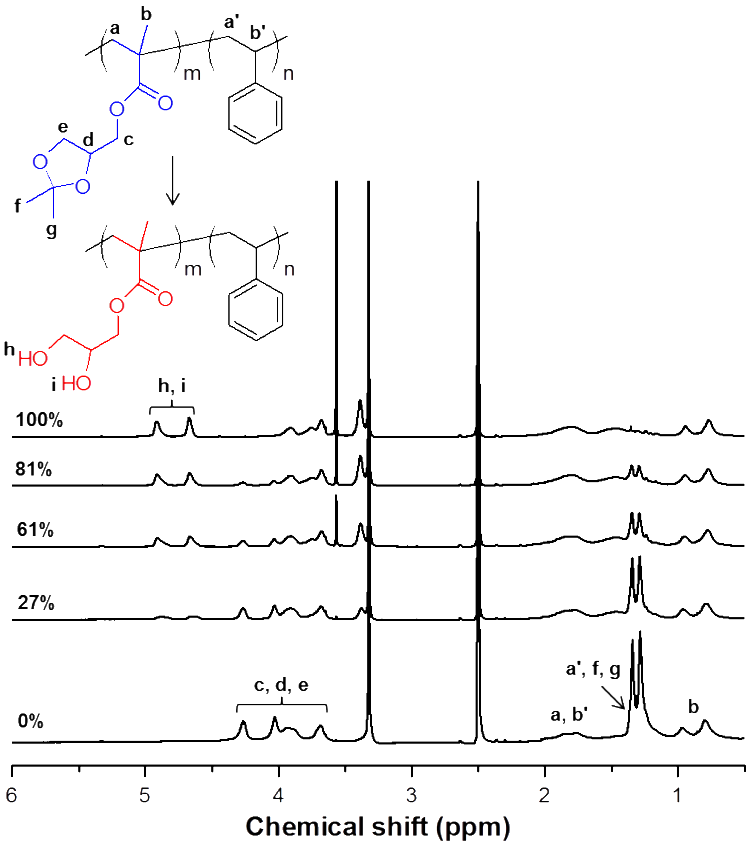

Figure S2. ^{1}H NMR spectra in DMSO-d_6 of P(SM13-S14) as a function of the degree of conversion calculated by the ratio of the peak areas between the methyl group of the backbone (*b*; 0.65−1.05 ppm) in SM segments and the hydroxy group (*h, i*; 4.55−4.96 ppm) in GM segments. The spectrums are vertically shifted for clarity.

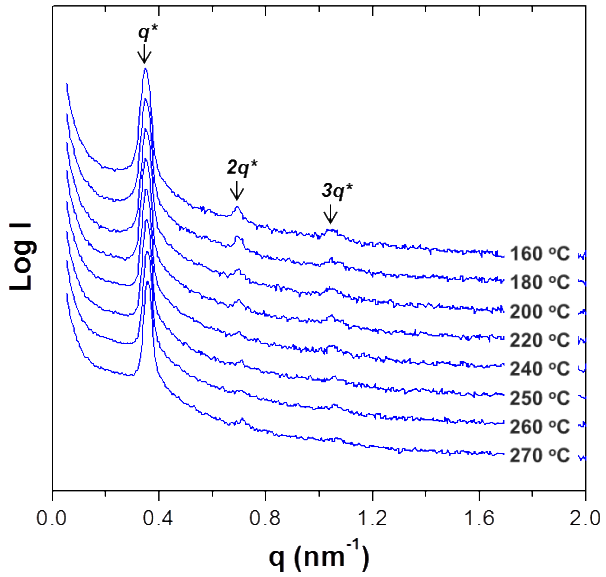

Figure S3. SAXS absolute intensity profiles for P(SM13-S14) of 27% conversion (N = 197) at various temperatures with a heating rate of 1.0 °C/min. The temperature-dependent profiles are vertically shifted in the range of 160 °C to 270 °C. The q* and higher order reflections (2q* and 3q*) of the lamellar structure were observed. Until 270 °C, the intensity at q* was not changed, indicating that P(SM13-S14) does not show a phase-mixed state and also maintains the condition of χN > 10.5 at 27% conversion due to the increase in χ.

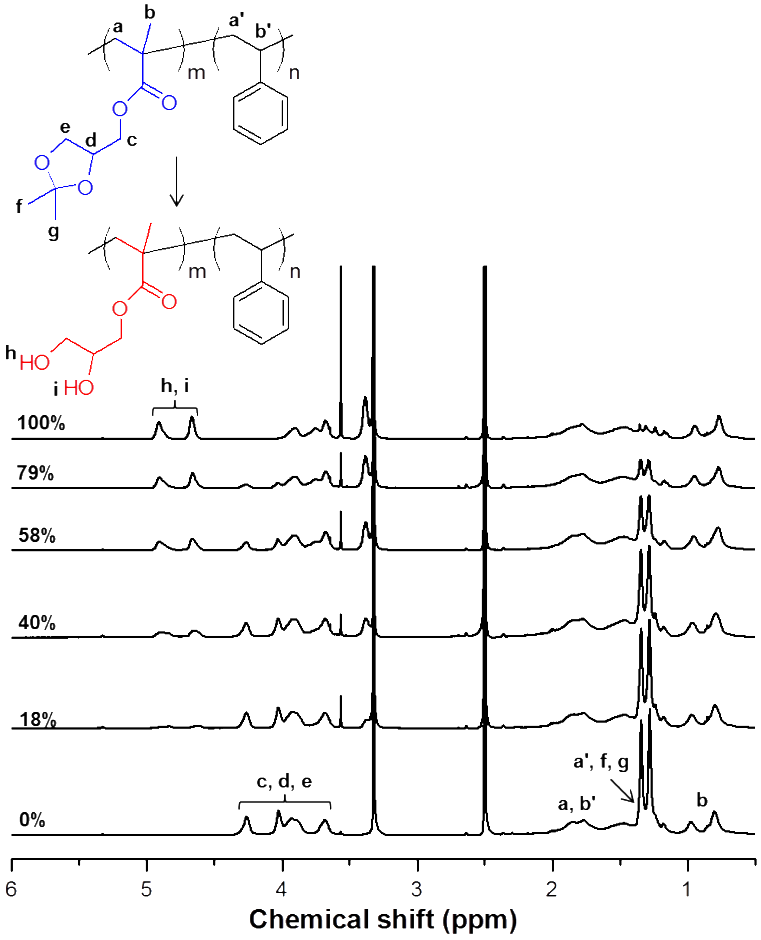

Figure S4. ^{1}H NMR spectra in DMSO-d_6 of P(SM5-S5) as a function of the degree of conversion calculated by the ratio of the peak areas between the methyl group of the backbone (*b*; 0.65−1.05 ppm) in SM segments and the hydroxy group (*h, i*; 4.55−4.96 ppm) in GM segments. The spectrums are vertically shifted for clarity.

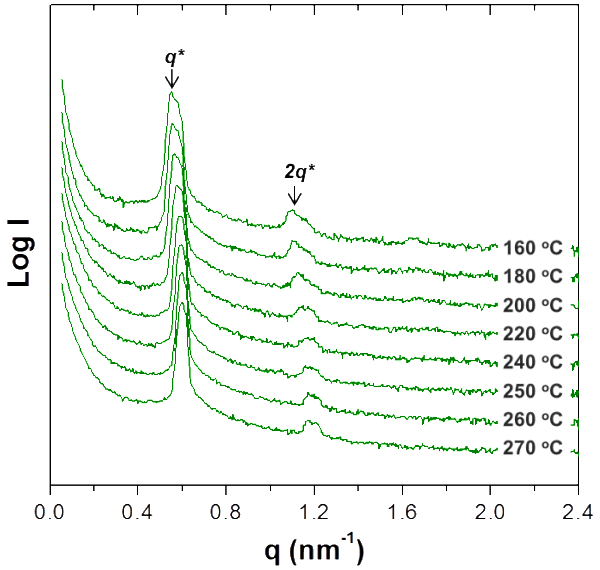

Figure S5. SAXS absolute intensity profiles for P(SM5-S5) of 58% conversion (N = 76) at various temperatures with a heating rate of 1.0 °C/min. The temperature-dependent profiles are vertically shifted in the range of 160 °C to 270 °C. The q* and higher order reflection (2q*) of the lamellar structure were observed. Until 270 °C, the intensity at q* was not changed, indicating that P(SM5-S5) does not show a phase-mixed state and also maintains the condition of χN > 10.5 at 58% conversion due to the increase in χ.

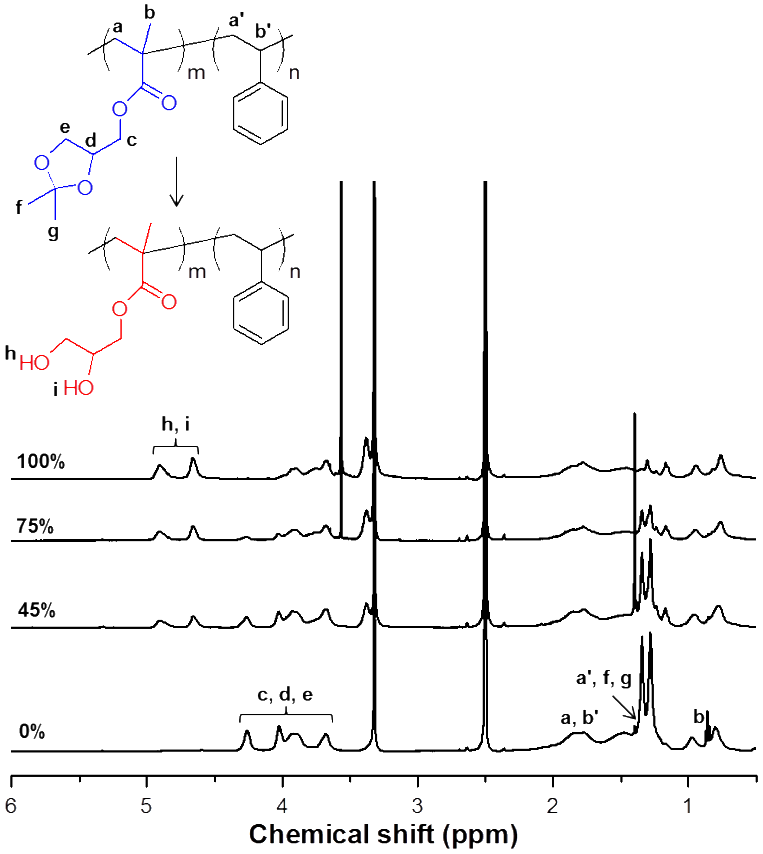

Figure S6. ^{1}H NMR spectra in DMSO-d_6 of P(SM2-S2) as a function of the degree of conversion calculated by the ratio of the peak areas between the methyl group of the backbone (*b*; 0.65−1.05 ppm) in SM segments and the hydroxy group (*h*, *i*; 4.55−4.96 ppm) in GM segments. The spectrums are vertically shifted for clarity.

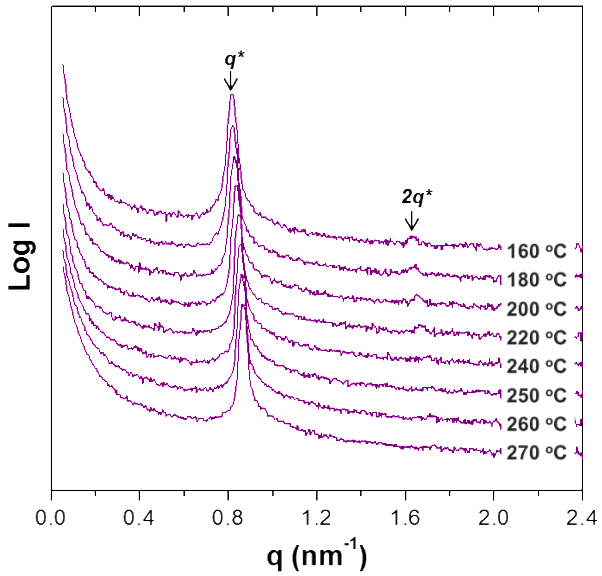

Figure S7. SAXS absolute intensity profiles for P(SM2-S2) of 100% conversion (N = 30) at various temperatures with a heating rate of 1.0 °C/min. The temperature-dependent profiles are vertically shifted in the range of 160 °C to 270 °C. The q^* and higher order reflection ($2q^*$) of the lamellar structure were observed. Until 270 °C, the q^* intensity was not changed, indicating that P(SM2-S2) does not show a phase-mixed state and also maintains the condition of $\chi N > 10.5$ at 100% conversion due to the increase in χ.

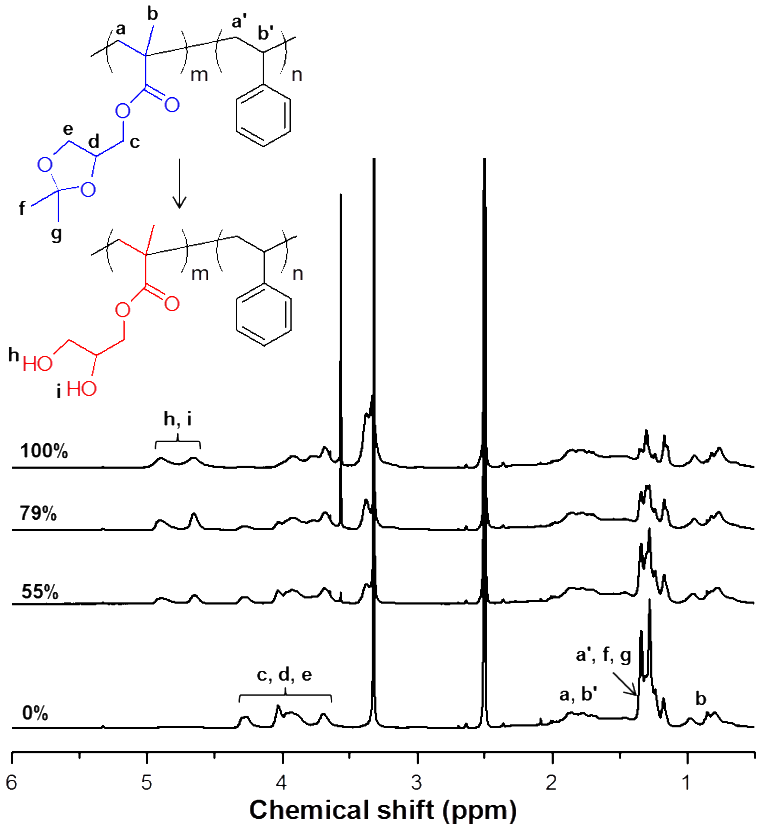

Figure S8. ^{1}H NMR spectra in DMSO-d_6 of P(SM1-S1) as a function of the degree of conversion calculated by the ratio of the peak areas between the methyl group of the backbone (*b*; 0.65−1.05 ppm) in SM segments and the hydroxy group (*h, i*; 4.55−4.96 ppm) in GM segments. The spectrums are vertically shifted for clarity.

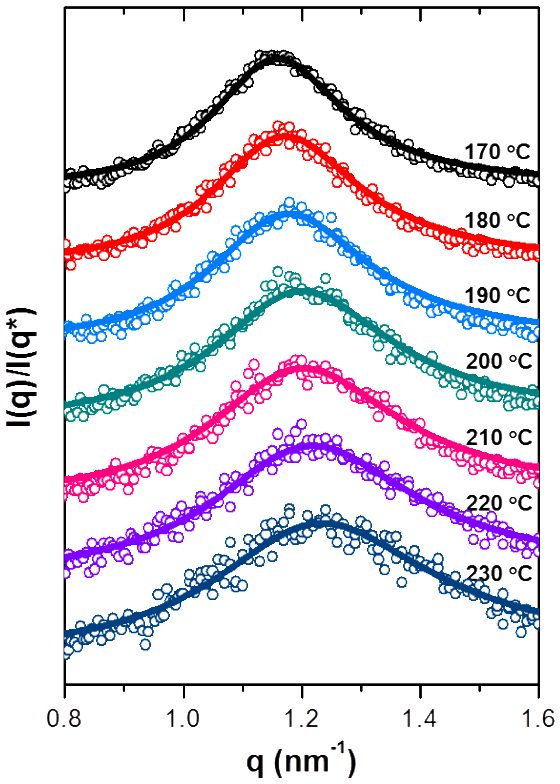

Figure S9. The scattering intensity profiles ($I(q)$) divided by the maximum intensity at q^* ($I(q^*)$) for P(SM1-S1) of 100% conversion (N = 16) at various temperatures over T_{ODT} (circle). The temperature-dependent profiles from 170 °C to 230 °C are shown, vertically shifted for clarity. By nonlinear regression analysis using $I(q)/I(q^*) = (F(q^*) - 2\chi)/(F(q) - 2\chi)$,[1-3] the χ value can be obtained at each temperature, where $F(q)$ is the interference function consisting of the Debye scattering function for individual blocks. The lines in the figure indicate the calculated scattering profiles from the equation fit to the experimental profiles.

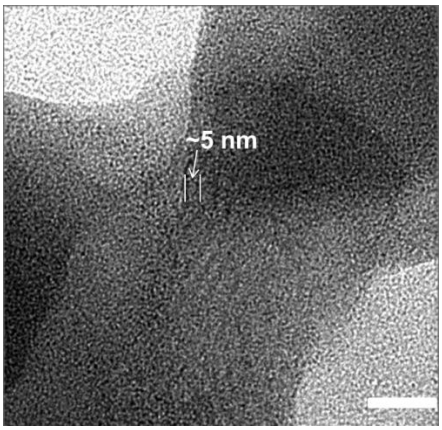

Figure S10. TEM image of P(GM1-S1) in bulk. The sample was microtomed into 20 nm thick films using a Leica Ultra Microtome at room temperature after thermal annealing at 140 °C for 24 h. Then, it was stained by exposure to RuO_4 vapor for 20 min. TEM measurements were performed using a JEOL 2200FS TEM at an accelerating voltage of 200 kV. The ~5 nm spacing of the lamellar microdomains were observed as the smallest domain spacing. Since RuO_4 is able to stain polymers having aromatic nucleus as well as hydroxyl groups,[4] the contrast between two lamellar microdomains was not exceptional but sufficient to observe the microdomains. The scale bar is 20 nm.

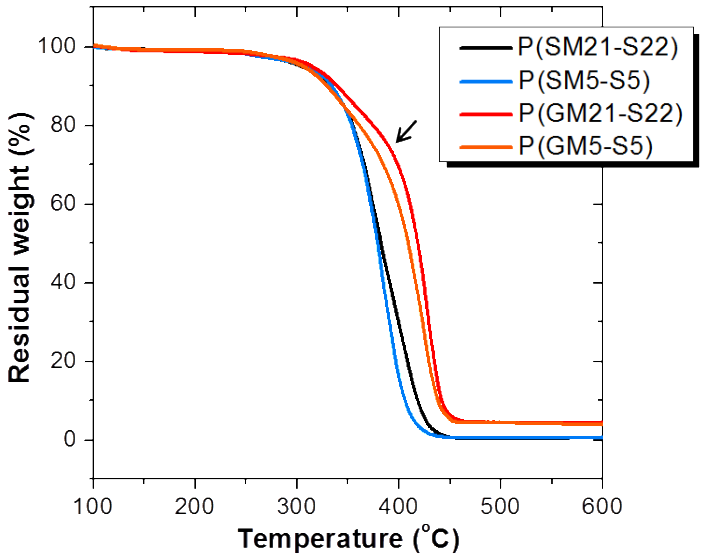

Figure S11. TGA curves for PSM-*b*-PS and PGM-*b*-PS copolymers, P(SM21-S22), P(SM5-S5), P(GM21-S22), and P(GM5-S5). The samples were measured at a heating rate of 10 °C/min under nitrogen gas from 100 °C to 700 °C. All copolymers showed that the thermal degradation began at ~270 °C and finished at ~450 °C. In contrast to the PSM-*b*-PS copolymers, the PGM-*b*-PS copolymers showed a two-step thermal degradation, due to the hydroxy groups on the side chain of the PGM block.[5,6] The first step at ~270 °C arose from the decomposition of the polymer backbone (depolymerization) and the second step at ~400 °C (arrow) is attributed to intramolecular side-chain reactions by the dehydration and cyclization of the hydroxy group.

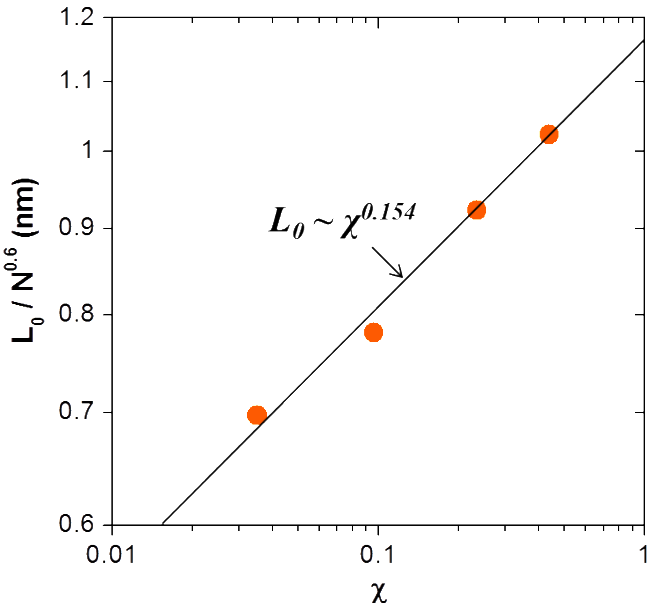

Figure S12. Scaling result of the PSM-*b*-PS copolymer between the domain spacing divided by degree of polymerization ($L_0/N^{0.6}$) and the χ value. Previously, we reported the relationship between L_0 and N in the strong segregation regime and it followed $L_0 \sim N^{0.6}$ for both PSM-*b*-PS and PGM-*b*-PS copolymers.[7] Therefore, we assumed that the randomly hydrolyzed PSM-*b*-PS copolymers also have the same scaling exponent as 0.6. In this manuscript, we evaluated the χ values at 0%, 40%, 75%, and 100% conversion. Since each χ value was calculated for different molecular weight samples, L_0 was divided by $N^{0.6}$ to get the relationship between L_0 and χ ($L_0/N^{0.6} \sim \chi^{\nu}$). The scaling exponent (ν) for L_0 and χ was found to be 0.154, similar to the theoretical value (ν = ~0.167). The graph is plotted on a log−log scale.

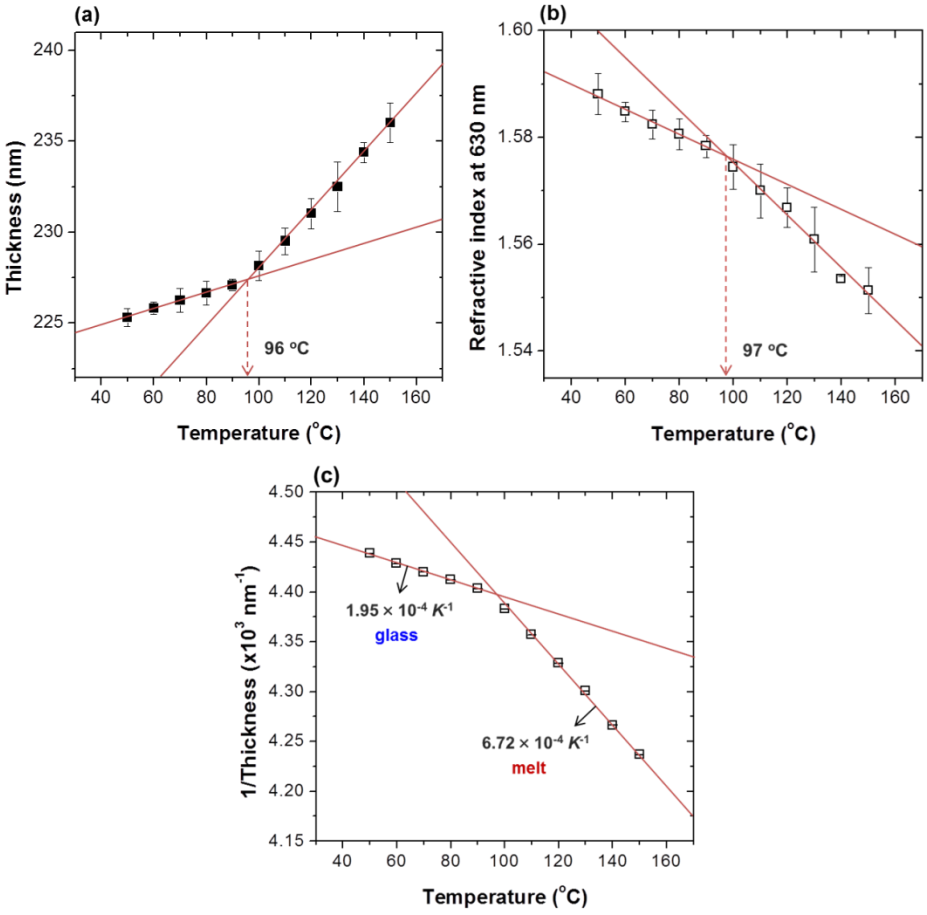

Figure S13. Thermal properties of a PS homopolymer. The sample was spin-coated on a silicon wafer with ~225 nm thickness. (a) The thickness and (b) refractive index of the polymer thin films as a function of temperature were determined from spectroscopic measurement (Filmetrics F20) with a heating stage (Linkam Scientific). The temperature of the samples on the heating stage was calibrated using a K-type digital thermometer. The refractive index of PS, obtained at 630 nm wavelength, was ~1.59 at 25 °C. From a change in the slope of the two linear fits to the thickness data, the glass transition temperature (T_g) of PS was observed at 96 °C and the similar value (97 °C) was seen at the refractive data. (c) Thermal expansion coefficient is defined as $\alpha \approx$

$-t_{avg}(d(1/t)/dT)$, where t_{avg} indicates the average film thickness.[8] Using this equation, the α values of PS at glass ($1.95 \times 10^{-4}\ K^{-1}$) and melt ($6.72 \times 10^{-4}\ K^{-1}$) states were determined.

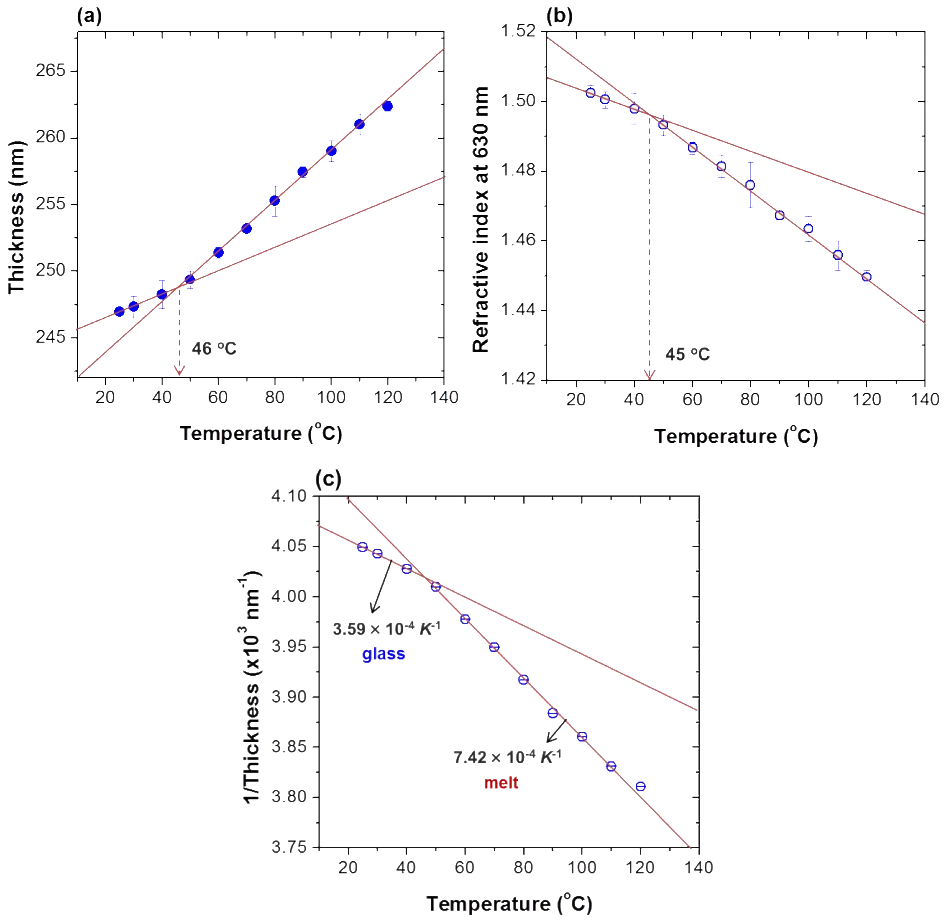

Figure S14. Thermal properties of a PSM homopolymer. The sample was spin-coated on a silicon wafer with ~246 nm thickness. (a) The thickness and (b) refractive index of the polymer thin films as a function of temperature were determined by the same instruments as mentioned in Figure S10. The refractive index of PSM, obtained at 630 nm wavelength, was ~1.51 at 25 °C. From a change in the slope of the two linear fits to the thickness data, the T_g of PSM was observed at 46 °C and the similar value (45 °C) was seen at the refractive data. (c) The α values of PSM at glass and melt states, which is higher than that of PS, were $3.59 \times 10^{-4}\ K^{-1}$ and $7.42 \times 10^{-4}\ K^{-1}$, respectively.

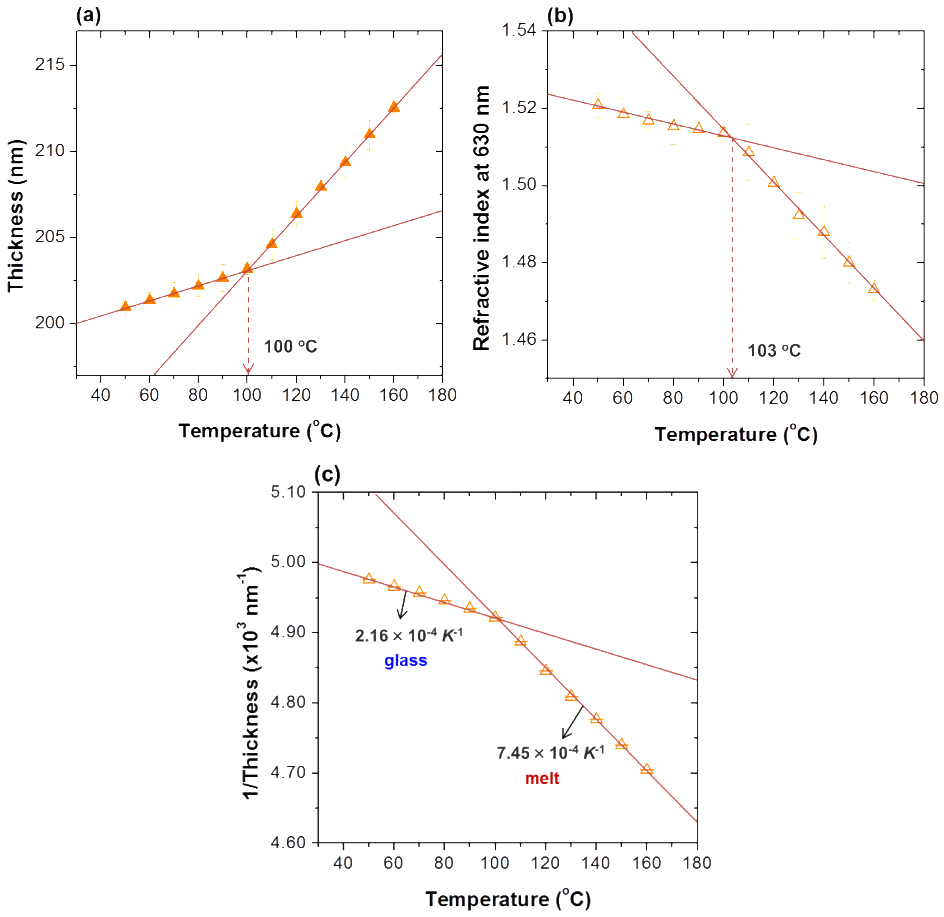

Figure S15. Thermal properties of a PGM homopolymer. The samples were prepared by exposing a spin-coated PSM thin film to trifluoroacetic acid (TFA) vapor for 10 min. (a) The thickness and (b) refractive index of the polymer thin films as a function of temperature were determined by the same instruments as mentioned in Figure S10. The refractive index of PGM, obtained at 630 nm wavelength, was ~1.52 at 25 °C. From a change in the slope of the two linear fits to the thickness and refractive data, PGM showed a higher T_g (~100 °C) than that of PSM due to the strong hydrogen bonding. (c) The α value of PGM at glass state ($2.16 \times 10^{-4}\ K^{-1}$) was lower, but it became similar to PSM at melt state ($7.45 \times 10^{-4}\ K^{-1}$).

Reference

[1] Leibler, L. Theory of Microphase Separation in Block Copolymers. *Macromolecules* **1980**, 13, 1602-1617.

[2] Russell, T. P.; Hjelm Jr, R. P.; Seeger, P. A. Temperature Dependence of the Interaction Parameter of Polystyrene and Poly(methyl methacrylate). *Macromolecules* **1990**, 23, 890-893.

[3] Ahn, H.; Ryu, D. Y.; Kim, Y.; Kwon, K. W.; Lee, J.; Cho, J. Phase Behavior of Polystyrene-*b*-poly(methyl methacrylate) Diblock Copolymer. *Macromolecules* **2009**, 42, 7897-7902.

[4] Trent, J. S.; Scheinbeim, J. I.; Couchman, P. R. Ruthenium Tetraoxide Staining of Polymers for Electron Micorscopy. *Macromolecules* **1983**, 16, 589-598.

[5] Kyerematen, S. O.; Amado, E.; Kressler, J. Synthesis and Characterization of Random Copolymers of (2,2-Dimethyl-1,3-dioxolan-4-yl)methyl Methacrylate and 2,3-Dihydroxypropyl Methacrylate. *Eur. Polym. J.* **2007**, 43, 3380-3391.

[6] Demirelli, K.; Coskun, M.; Kaya, E. A Detailed Study of Theraml Degradation of Poly(2-hydroxyethyl methacrylate). *Polym. Degrad. Stab.* **2001**, 72, 75-80.

[7] Jeong, G.; Yu, D. M.; Mapas, J. K. D.; Sun, Z.; Rzayev, J.; Russell, T. P. Realizing 5.4 nm Full Pitch Lamellar Microdomains by a Solid-State Transformation. *Macromolecules* **2017**, 50, 7148-7154.

[8] Beaucage, G.; Composto, R.; Stein, R. S. Ellipsometric Study of the Glass Transition and Thermal Expansion Coefficients of Thin Polymer Films. *J. Polym. Sci. B Polym. Phys.* **1993**, 319-326.